QCD Corrections to $b \to s\gamma$ Decay in 2-Higgs Doublet Model

Cai-Dian Lü*

CCAST(World Laboratory), P.O.Box 8730, Beijing 100080, China

Institute of Theoretical Physics, Academia Sinica, P.O.Box 2735,

Beijing 100080, China†

August 16, 1994

Abstract

We give a more complete calculation of $b \to s\gamma$ decay in 2-Higgs doublet model, including leading log QCD corrections from m_{top} to M_W in addition to corrections from M_W to m_b. The inclusive decay rate in the first model is found to be suppressed 23% comparing with the calculations without the QCD running from m_{top} to M_W. And the enhancement up to 5% is found in calculations of the second model. More strict restrictions to parameters of 2-Higgs doublet model II are found.

*E-mail: lucd@itp.ac.cn.

†Mailing address.

1 Introduction

The standard model(SM) has achieved a great success recent years. However, there is still a vast interest beyond standard model. One of the most simple extensions of the standard model is to add another Higgs doublet. This may be viewed as inevitable since many attempts at going beyond the SM leads to an enlargement of the Higgs sector (Such as Supersymmetry Model). It is of interest to study the 2-Higgs doublet model, hence to constrain other models.

The decay $b \to s\gamma$ is one of the very useful channel for study of models beyond standard model[1]. Recently the CLEO collaboration has observed[2] the exclusive decay $B \to K^*\gamma$ with a branching fraction of $(4.5 \pm 1.5 \pm 0.9) \times 10^{-5}$. A new upper limit on the inclusive $b \to s\gamma$ process is also obtained as $B(b \to s\gamma) < 5.4 \times 10^{-4}$ at 95% C.L.[3]. This leads to a number of papers[4] regarding this decay recently. It has been argued that the experimental result is more close to standard model predictions and provides more information about restrictions on models beyond SM. This deeply depends on more precise calculations of this decay. The decay of $b \to s\gamma$ and its large leading log QCD corrections have already been calculated in many papers[5, 6, 7, 8, 9]. Due to many reasons, there are discrepancies among these papers, although there is not much differences in numerical results. Until recently, Ciuchini, Franco, Reina and Silvestrini[10] performed this calculation in three regularization schemes, to solve this problem completely. And also some efforts are made to give a next to leading log calculations[11, 12] which is estimated within 20% contribution. All these efforts make it easy for calculations of this decay in models beyond SM.

The radiative b quark decay in 2-Higgs doublet model has also been calculated in several papers[5, 13, 14, 15]. It is found to be strongly QCD-enhanced. In other words, the strong

interaction plays an important role in this decay. However, there are still some uncertainties in these papers. All these papers do not include the QCD running from m_{top} to M_W. Since the top quark is found to be 2-times heavier than W boson($m_{top} = 174 \pm 10^{+13}_{-12}$ GeV [16]), and the charged Higgs is also expected to be heavier(in supersymmetry model $m_\phi^2 = M_W^2 + m_A^2$), it needs a detailed calculation of this effect.

In our present paper, by using effective field theory formalism, we recalculate the $b \to s\gamma$ decay in 2-Higgs doublet model including QCD running from m_{top} to M_W, in addition to corrections from M_W to m_b, so as to give a complete leading log results. In the next section, we first integrate out the top quark and charged Higgs, generating an effective five-quark theory. By using the renormalization group equation, we run the effective field theory down to the W-scale. In section 3, the weak bosons are removed. Then we continue running the effective field theory down to b-quark scale to include QCD corrections from M_W to m_b. In section 4, the rate of radiative b decay is obtained. Restrictions of model parameters from experiments of CLEO collaboration are also given. Section 5 is a short summary.

2 QCD Corrections from $\mu = m_{top}$ to $\mu = M_W$ Scale

With two Higgs doublets, one has to avoid tree-level flavor changing neutral currents (FCNCs) due to neutral Higgs bosons. This is usually achieved in two ways, each involving some discrete symmetry. the first way (model I) is to allow only one Higgs doublet to couple to both types of quarks[17]. The second way (model II) is to couple only one Higgs doublet to u-type quarks while the other couples only to d-type quarks[18]. It is of interest to note that model II occurs as a natural feature in theories with supersymmetry or a Peccei-Quinn type of symmetry.

The Lagrangian of the 2-Higgs doublet Model is

$$\begin{aligned}\mathcal{L} &= \frac{1}{\sqrt{2}}\frac{\mu^{\epsilon/2}g_2}{M_W}\left[\left(\frac{v_2}{v_1}\right)\left(\begin{array}{ccc}\overline{u} & \overline{c} & \overline{t}\end{array}\right)_R M_U V \left(\begin{array}{c} d \\ s \\ b \end{array}\right)_L - \xi\left(\begin{array}{ccc}\overline{u} & \overline{c} & \overline{t}\end{array}\right)_L V M_D \left(\begin{array}{c} d \\ s \\ b \end{array}\right)_R\right] H_+ \\ &+ h.c. \\ &+ \cdots. \end{aligned} \tag{1}$$

Where V represents the 3×3 unitary Kobayashi-Maskawa matrix, M_U and M_D denote the diagonalized quark mass matrices, the subscript L and R denote left-handed and right-handed quarks, respectively. For model I, $\xi = v_2/v_1$; while for Model II, $\xi = -v_1/v_2$. And v_1, v_2 are the magnitude of the vacuum expectation values of two Higgs doublets, respectively. To keep explicit gauge invariance, we work in a background field gauge[19].

At first, we integrate out the top quark and charged Higgs, generating an effective five quark theory, introducing dimension-6 effective operators as to include effects of the absent top quark and charged Higgs. Higher dimension operators are suppressed by factor of p^2/m_t^2, where p^2 characterizing the interesting external momentum of b quark $p^2 \sim m_b^2$. For leading order of m_b^2/m_t^2, dimension-6 operators are good enough to make a complete basis of operators:

$$\begin{aligned} O_{LR}^1 &= -\frac{1}{16\pi^2} m_b \overline{s}_L D^2 b_R, \\ O_{LR}^2 &= \mu^{\epsilon/2}\frac{g_3}{16\pi^2} m_b \overline{s}_L \sigma^{\mu\nu} X^a b_R G_{\mu\nu}^a, \\ O_{LR}^3 &= \mu^{\epsilon/2}\frac{eQ_b}{16\pi^2} m_b \overline{s}_L \sigma^{\mu\nu} b_R F_{\mu\nu}, \\ Q_{LR} &= \mu^{\epsilon} g_3^2 m_b \phi_+ \phi_- \overline{s}_L b_R, \\ P_L^{1,A} &= -\frac{i}{16\pi^2} \overline{s}_L T_{\mu\nu\sigma}^A D^\mu D^\nu D^\sigma b_L, \\ P_L^2 &= \mu^{\epsilon/2}\frac{eQ_b}{16\pi^2} \overline{s}_L \gamma^\mu b_L \partial^\nu F_{\mu\nu}, \end{aligned}$$

$$
\begin{aligned}
P_L^3 &= \mu^{\epsilon/2}\frac{eQ_b}{16\pi^2}F_{\mu\nu}\overline{s}_L\gamma^\mu D^\nu b_L,\\
P_L^4 &= i\mu^{\epsilon/2}\frac{eQ_b}{16\pi^2}\tilde{F}_{\mu\nu}\overline{s}_L\gamma^\mu\gamma^5 D^\nu b_L,\\
R_L^1 &= i\mu^\epsilon g_3^2\phi_+\phi_-\overline{s}_L \not{D} b_L,\\
R_L^2 &= i\mu^\epsilon g_3^2(D^\sigma\phi_+)\phi_-\overline{s}_L\gamma_\sigma b_L,\\
R_L^3 &= i\mu^\epsilon g_3^2\phi_+(D^\sigma\phi_-)\overline{s}_L\gamma_\sigma b_L,\\
W_{LR} &= -i\mu^\epsilon g_3^2 m_b W_+^\nu W_-^\mu\overline{s}_L\sigma_{\mu\nu}b_R,\\
W_L^1 &= i\mu^\epsilon g_3^2 W_+^\nu W_-^\mu\overline{s}_L\gamma_\mu \not{D}\gamma_\nu b_L,\\
W_L^2 &= i\mu^\epsilon g_3^2(D^\sigma W_+^\nu)W_-^\mu\overline{s}_L\gamma_\mu\gamma_\sigma\gamma_\nu b_L,\\
W_L^3 &= i\mu^\epsilon g_3^2 W_{+\mu}W_-^\mu\overline{s}_L \overleftrightarrow{\not{D}} b_L,\\
W_L^4 &= i\mu^\epsilon g_3^2 W_+^\nu W_-^\mu\overline{s}_L(\overleftrightarrow{D}_\mu\gamma_\nu+\gamma_\mu\overleftrightarrow{D}_\nu)b_L.
\end{aligned}
\tag{2}
$$

Where $\overline{s}_L\overleftrightarrow{D}_\mu\gamma_\nu b_L$ stands for $(\overline{s}_L D_\mu\gamma_\nu b_L+(D_\mu\overline{s}_L)\gamma_\nu b_L)$ and the covariant derivative is defined as

$$
D_\mu=\partial_\mu-i\mu^{\epsilon/2}g_3X^aG_\mu^a-i\mu^{\epsilon/2}eQA_\mu,
$$

with g_3 denoting the QCD coupling constant. The tensor $T^A_{\mu\nu\sigma}$ appearing in $P_L^{1,A}$ assumes the following Lorentz structure, the index A ranging from 1 to 4:

$$
\begin{aligned}
T^1_{\mu\nu\sigma}&=g_{\mu\nu}\gamma_\sigma,\quad T^2_{\mu\nu\sigma}=g_{\mu\sigma}\gamma_\nu,\\
T^3_{\mu\nu\sigma}&=g_{\nu\sigma}\gamma_\mu,\quad T^4_{\mu\nu\sigma}=-i\epsilon_{\mu\nu\sigma\tau}\gamma^\tau\gamma_5.
\end{aligned}
\tag{3}
$$

Then we can write down our effective Hamiltonian as

$$
\mathcal{H}_{eff}=2\sqrt{2}G_F V_{tb}V_{ts}^*\sum_i C_i(\mu)O_i(\mu).
\tag{4}
$$

The coefficients $C_i(\mu)$ can be calculated from matching diagrams displayed in Fig.1 and Fig.2. Calculating left hand side of Fig.1, keeping only leading orders of p^2/m_t^2, we get coefficients of

right hand side operators:

$$\begin{aligned} C_{R^1_L} &= C_{R^2_L} = -C_{Q_{LR}} = 1/g_3^2, \\ C_{R^3_L} &= 0, \\ C_{W_{LR}} &= C_{W^3_L} = C_{W^4_L} = 0, \\ C_{W^1_L} &= C_{W^2_L} = \delta/g_3^2. \end{aligned} \tag{5}$$

In Fig.2, coefficients of right hand side operators are all from the finite part integrations of left side electroweak loops. Terms like $\log(\mu^2/m_t^2)$ vanish here, because of the matching scale $\mu = m_t$. They will be regenerated by renormalization group running of electroweak later. After calculation one has

$$\begin{aligned}
C_{O^1_{LR}} &= -\left(\frac{1+\delta}{2(1-\delta)^2} + \frac{\delta}{(1-\delta)^3}\log\delta\right) - \xi'\left(\frac{1+x}{2(1-x)^2} + \frac{x}{(1-x)^3}\log x\right), \\
C_{O^2_{LR}} &= -\frac{1}{2}\left(\frac{1}{(1-\delta)} + \frac{\delta}{(1-\delta)^2}\log\delta\right) - \xi'\left(\frac{1}{2(1-x)} + \frac{x}{2(1-x)^2}\log x\right), \\
C_{O^3_{LR}} &= \left(\frac{1}{(1-\delta)} + \frac{\delta}{(1-\delta)^2}\log\delta\right) + \xi\left(\frac{1}{1-x} + \frac{x}{(1-x)^2}\log x\right), \\
C_{P^{1,1}_L} &= C_{P^{1,3}_L} = \left(\frac{\frac{11}{18} + \frac{5}{6}\delta - \frac{2}{3}\delta^2 + \frac{2}{9}\delta^3}{(1-\delta)^3} + \frac{\delta + \delta^2 - \frac{5}{3}\delta^3 + \frac{2}{3}\delta^4}{(1-\delta)^4}\log\delta\right) \\
&\quad + \left(\frac{v_2}{v_1}\right)^2\left(\frac{\frac{11}{18} - \frac{7}{18}x + \frac{1}{9}x^2}{(1-x)^3} + \frac{x - x^2 + \frac{1}{3}x^3}{(1-x)^4}\log x\right), \\
C_{P^{1,2}_L} &= \left(\frac{-\frac{8}{9} - \frac{1}{6}\delta + \frac{17}{6}\delta^2 - \frac{7}{9}\delta^3}{(1-\delta)^3} + \frac{-\delta + \frac{10}{3}\delta^3 - \frac{4}{3}\delta^4}{(1-\delta)^4}\log\delta\right) \\
&\quad + \left(\frac{v_2}{v_1}\right)^2\left(\frac{-\frac{8}{9} + \frac{29}{18}x - \frac{7}{18}x^2}{(1-x)^3} + \frac{-x + 2x^2 - \frac{2}{3}x^3}{(1-x)^4}\log x\right), \\
C_{P^{1,4}_L} &= \left(\frac{\frac{1}{2} - \delta - \frac{1}{2}\delta^2 + \delta^3}{(1-\delta)^3} + \frac{\delta - 3\delta^2 + 2\delta^3}{(1-\delta)^4}\log\delta\right) \\
&\quad + \left(\frac{v_2}{v_1}\right)^2\left(\frac{1-x^2}{2(1-x)^3} + \frac{x-x^2}{(1-x)^4}\log x\right), \\
C_{P^2_L} &= \frac{1}{Q_b}\left(\frac{\frac{3}{4} + \frac{1}{2}\delta - \frac{7}{4}\delta^2 + \frac{1}{2}\delta^3}{(1-\delta)^3} - \frac{1}{3}\delta + \left(\frac{\frac{1}{6} + \frac{5}{6}\delta - \frac{5}{3}\delta^3 + \frac{2}{3}\delta^4}{(1-\delta)^4} - \frac{1}{6} - \frac{1}{3}\delta\right)\log\delta\right) \\
&\quad + \frac{1}{Q_b}\left(\frac{v_2}{v_1}\right)^2\left(\frac{\frac{3}{4} - x + \frac{1}{4}x^2}{(1-x)^3} + \frac{\frac{1}{6} + \frac{1}{2}x - x^2 + \frac{1}{3}x^3}{(1-x)^4}\log x\right),
\end{aligned}$$

$$
\begin{aligned}
C_{P_L^3} &= 0, \\
C_{P_L^4} &= \frac{1}{Q_b}\left(\frac{-\frac{1}{2}-5\delta+\frac{17}{2}\delta^2-3\delta^3}{(1-\delta)^3}+\frac{-5\delta+7\delta^2-2\delta^3}{(1-\delta)^4}\log\delta+4\delta\log\delta\right) \\
&\quad -\frac{1}{Q_b}\left(\frac{v_2}{v_1}\right)^2\left(\frac{1-x^2}{2(1-x)^3}+\frac{x-x^2}{(1-x)^4}\log x\right). \qquad (6)
\end{aligned}
$$

Where $\delta = M_W^2/m_t^2$, $x = m_\phi^2/m_t^2$; With

$$\xi' = v_2^2/v_1^2, \qquad model\ I,$$

$$\xi' = -1, \qquad model\ II.$$

When $\xi = \xi' = 0$, the above result (6) reduces to that of SM case[20, 21].

The renormalization group equation satisfied by the coefficient functions $C_i(\mu)$ is

$$\mu\frac{d}{d\mu}C_i(\mu) = \sum_j(\gamma^\tau)_{ij}C_j(\mu). \qquad (7)$$

Where the anomalous dimension matrix γ_{ij} is calculated in practice by requiring renormalization group equations for Green functions with insertions of composite operators to be satisfied order by order in perturbation theory.

After evaluating the loop diagrams, we find the following leading order weak mixing of

operators, with the Q, R part agrees with ref.[20].

$$\gamma = \begin{array}{c} \\ Q_{LR} \\ R_L^1 \\ R_L^2 \\ R_L^3 \\ W_{LR} \\ W_L^1 \\ W_L^2 \\ W_L^3 \\ W_L^4 \end{array} \begin{array}{c} \begin{array}{ccccccc} O_{LR}^1 & O_{LR}^2 & O_{LR}^3 & P_L^{1,A} & P_L^2 & P_L^3 & P_L^4 \end{array} \\ \begin{pmatrix} 0 & 0 & 0 & 0 & 0 & 0 & 0 \\ 0 & 0 & 0 & 0 & 0 & 0 & 0 \\ 0 & 0 & 0 & 0 & -1/2 & 0 & 0 \\ 0 & 0 & 0 & 0 & 1/2 & 0 & 0 \\ 0 & 0 & 6 & 0 & 0 & 0 & 0 \\ 0 & 0 & 0 & 0 & 0 & 0 & 12 \\ 0 & 0 & 0 & 0 & -1 & 0 & 0 \\ 0 & 0 & 0 & 0 & 0 & 0 & 0 \\ 0 & 0 & 0 & 0 & 0 & 0 & 0 \end{pmatrix} \end{array} \quad 16\pi^2 \, \frac{g_3^2}{8\pi^2}. \tag{8}$$

These mixing are all between operators induced by tree-diagrams and operators induced by loop-diagrams. The vanishing $\log(\mu^2/m_t^2)$ terms in previous matching are regenerated here by renormalization group equation(7).

The QCD anomalous dimensions for each of the operators in our basis are

$$\gamma = \begin{array}{c} \\ O^1_{LR} \\ O^2_{LR} \\ O^3_{LR} \\ P^{1,1}_L \\ P^{1,2}_L \\ P^{1,3}_L \\ P^{1,4}_L \\ P^2_L \\ P^3_L \\ P^4_L \end{array} \begin{array}{c} \begin{array}{cccccccccc} O^1_{LR} & O^2_{LR} & O^3_{LR} & P^{1,1}_L & P^{1,2}_L & P^{1,3}_L & P^{1,4}_L & P^2_L & P^3_L & P^4_L \end{array} \\ \begin{pmatrix} \frac{20}{3} & 1 & -2 & 0 & 0 & 0 & 0 & 0 & 0 & 0 \\ -8 & \frac{2}{3} & \frac{4}{3} & 0 & 0 & 0 & 0 & 0 & 0 & 0 \\ 0 & 0 & \frac{16}{3} & 0 & 0 & 0 & 0 & 0 & 0 & 0 \\ 6 & 2 & -1 & \frac{2}{3} & 2 & -2 & -2 & 0 & 0 & 0 \\ 4 & \frac{3}{2} & 0 & -\frac{113}{36} & \frac{137}{18} & -\frac{113}{36} & -\frac{4}{3} & \frac{9}{4} & 0 & 0 \\ 2 & 1 & 1 & -2 & 2 & \frac{2}{3} & -2 & 0 & 0 & 0 \\ 0 & \frac{1}{2} & 2 & -\frac{113}{36} & \frac{89}{18} & -\frac{113}{36} & \frac{4}{3} & \frac{9}{4} & 0 & 0 \\ 0 & 0 & 0 & 0 & 0 & 0 & 0 & 0 & 0 & 0 \\ 0 & 0 & -\frac{4}{3} & 0 & 0 & 0 & 0 & 0 & 0 & 0 \\ 0 & 0 & -\frac{4}{3} & 0 & 0 & 0 & 0 & 0 & 0 & 0 \end{pmatrix} \end{array} \frac{g_3^2}{8\pi^2}, \tag{9}$$

$$\gamma = \begin{array}{c} \\ Q_{LR} \\ R^1_L \\ R^2_L \\ R^3_L \\ W_{LR} \\ W^1_L \\ W^2_L \\ W^3_L \\ W^4_L \end{array} \begin{array}{c} \begin{array}{ccccccccc} Q_{LR} & R^1_L & R^2_L & R^3_L & W_{LR} & W^1_L & W^2_L & W^3_L & W^4_L \end{array} \\ \begin{pmatrix} \frac{23}{3} & 0 & 0 & 0 & 0 & 0 & 0 & 0 & 0 \\ 0 & \frac{23}{3} & 0 & 0 & 0 & 0 & 0 & 0 & 0 \\ 0 & 0 & \frac{23}{3} & 0 & 0 & 0 & 0 & 0 & 0 \\ 0 & 0 & 0 & \frac{23}{3} & 0 & 0 & 0 & 0 & 0 \\ 0 & 0 & 0 & 0 & 13 & 0 & 0 & 0 & 0 \\ 0 & 0 & 0 & 0 & -\frac{8}{3} & \frac{23}{3} & 0 & -\frac{8}{9} & \frac{16}{9} \\ 0 & 0 & 0 & 0 & 0 & 0 & \frac{23}{3} & 0 & 0 \\ 0 & 0 & 0 & 0 & 0 & 0 & 0 & \frac{23}{3} & 0 \\ 0 & 0 & 0 & 0 & 0 & 0 & 0 & -\frac{16}{9} & \frac{101}{9} \end{pmatrix} \end{array} \frac{g_3^2}{8\pi^2}. \tag{10}$$

The mixing elements between the two matrix (9) and (10) are all zero in leading log approximation. There are some differences in the anomalous dimension matrix comparing with Cho and Grinstein's result[20]. If we omit a symmetric factor of 1/2 in calculating Feynman diagram like Fig.3, the results will agree with them[21]. But according to similar diagram calculation like ref.[9, 10], this factor can not be omitted. For instance, diagram like Fig. 3 is also appeared in calculation of anomalous dimension of the gluon magnetic moment-type operator O_8 in ref.[9, 10] with a symmetric factor 1/2. This is also shown in general Feynman gauge calculation, and it give results same as the above. After these changes, the whole matrix can be easily diagonalized, and gives all real eigenvalues, which is required to maintain hermiticity of the effective hamiltonian at all renormalization scales. While in ref.[20], it can not. In their case, some eigenvalues are complex.

The solution to renormalization group equation (7) appears in obvious matrix notation as

$$C(\mu_2) = \left[\exp \int_{g_3(\mu_1)}^{g_3(\mu_2)} dg \frac{\gamma^T(g)}{\beta(g)}\right] C(\mu_1). \tag{11}$$

After inserting anomalous dimension (8–10), we can have the coefficients of operators at $\mu = M_W$.

3 QCD Corrections from $\mu = M_W$ to $\mu = m_b$ Scale

In order to continue running the basis operator coefficients down to lower scales, one must integrate out the weak gauge bosons and would-be Goldstone bosons at $\mu = M_W$ scale. The diagrams are displayed in Fig.4. From the second and third matching equations of this figure, one finds the following relations between coefficient functions just below(-) and above(+) $\mu = M_W$:

$$C_{O^1_{LR}}(M_W^-) \;=\; C_{O^1_{LR}}(M_W^+),$$

$$
\begin{aligned}
C_{O^2_{LR}}(M_W^-) &= C_{O^2_{LR}}(M_W^+), \\
C_{O^3_{LR}}(M_W^-) &= C_{O^3_{LR}}(M_W^+), \\
C_{P_L^{1,1}}(M_W^-) &= C_{P_L^{1,1}}(M_W^+) + 2/9, \\
C_{P_L^{1,2}}(M_W^-) &= C_{P_L^{1,2}}(M_W^+) - 7/9, \\
C_{P_L^{1,3}}(M_W^-) &= C_{P_L^{1,3}}(M_W^+) + 2/9, \\
C_{P_L^{1,4}}(M_W^-) &= C_{P_L^{1,4}}(M_W^+) + 1, \\
C_{P_L^2}(M_W^-) &= C_{P_L^2}(M_W^+) - C_{W_L^2}(M_W^+) - 3/2, \\
C_{P_L^3}(M_W^-) &= C_{P_L^3}(M_W^+), \\
C_{P_L^4}(M_W^-) &= C_{P_L^4}(M_W^+) + 9.
\end{aligned} \tag{12}
$$

In addition to these, there are new four-quark operators from the first equation of Fig.4[5, 8, 10]:

$$
\begin{aligned}
O_1 &= (\overline{c}_{L\beta}\gamma^\mu b_{L\alpha})(\overline{s}_{L\alpha}\gamma_\mu c_{L\beta}), \\
O_2 &= (\overline{c}_{L\alpha}\gamma^\mu b_{L\alpha})(\overline{s}_{L\beta}\gamma_\mu c_{L\beta}), \\
O_3 &= (\overline{s}_{L\alpha}\gamma^\mu b_{L\alpha})[(\overline{u}_{L\beta}\gamma_\mu u_{L\beta}) + ... + (\overline{b}_{L\beta}\gamma_\mu b_{L\beta})], \\
O_4 &= (\overline{s}_{L\alpha}\gamma^\mu b_{L\beta})[(\overline{u}_{L\beta}\gamma_\mu u_{L\alpha}) + ... + (\overline{b}_{L\beta}\gamma_\mu b_{L\alpha})], \\
O_5 &= (\overline{s}_{L\alpha}\gamma^\mu b_{L\alpha})[(\overline{u}_{R\beta}\gamma_\mu u_{R\beta}) + ... + (\overline{b}_{R\beta}\gamma_\mu b_{R\beta})], \\
O_6 &= (\overline{s}_{L\alpha}\gamma^\mu b_{L\beta})[(\overline{u}_{R\beta}\gamma_\mu u_{R\alpha}) + ... + (\overline{b}_{R\beta}\gamma_\mu b_{R\alpha})],
\end{aligned} \tag{13}
$$

with coefficients

$$
C_i(M_W) = 0, \quad i = 1, 3, 4, 5, 6, \quad C_2(M_W) = 1.
$$

To simplify the calculation and compare with the previous results, equations of motion(EOM)[22] is used to reduce all the remaining two-quark operators to the gluon and photon magnetic mo-

ment operators O^2_{LR} and O^3_{LR}. To be comparable with previous results without QCD corrections from m_{top} to M_W, operators O^3_{LR}, O^2_{LR} are rewritten as O_7, O_8 like ref.[5, 8, 10],

$$\begin{aligned} O_7 &= (e/16\pi^2) m_b \overline{s}_L \sigma^{\mu\nu} b_R F_{\mu\nu}, \\ O_8 &= (g/16\pi^2) m_b \overline{s}_L \sigma^{\mu\nu} T^a b_R G^a_{\mu\nu}. \end{aligned} \tag{14}$$

Then

$$\begin{aligned} C_7(M_W^-) &= \frac{1}{3} C_{O^3_{LR}}(M_W^-), \\ C_8(M_W^-) &= -C_{O^2_{LR}}(M_W^-). \end{aligned} \tag{15}$$

The operator basis now consists of 8 operators. The effective Hamiltonian appears just below the W-scale as

$$\begin{aligned} \mathcal{H}_{eff} &= \frac{4G_F}{\sqrt{2}} V_{tb} V_{ts}^* \sum_i C_i(M_W^-) O_i(M_W^-) \\ &\overset{EOM}{\to} \frac{4G_F}{\sqrt{2}} V_{tb} V_{ts}^* \left\{ \sum_{i=1}^{6} C_i(M_W^-) O_i + C_7(M_W^-) O_7 + C_8(M_W^-) O_8 \right\}. \end{aligned} \tag{16}$$

For completeness, the explicit expressions of the coefficient of operator O_8 and O_7 at $\mu = M_W^-$ are given,

$$\begin{aligned} C_{O_8}(M_W^-) &= \left(\frac{\alpha_s(m_t)}{\alpha_s(M_W)} \right)^{\frac{14}{23}} \left\{ \frac{1}{2} C_{O^1_{LR}}(m_t) - C_{O^2_{LR}}(m_t) + \frac{1}{2} C_{P^{1,1}_L}(m_t) \right. \\ &\left. + \frac{1}{4} C_{P^{1,2}_L}(m_t) - \frac{1}{4} C_{P^{1,4}_L}(m_t) \right\} - \frac{1}{3}, \end{aligned} \tag{17}$$

$$\begin{aligned} C_{O_7}(M_W^-) = \frac{1}{3} \left(\frac{\alpha_s(m_t)}{\alpha_s(M_W)} \right)^{\frac{16}{23}} & \left\{ C_{O^3_{LR}}(m_t) + 8 C_{O^2_{LR}}(m_t) \left[1 - \left(\frac{\alpha_s(M_W)}{\alpha_s(m_t)} \right)^{\frac{2}{23}} \right] \right. \\ + \left[-\frac{9}{2} C_{O^1_{LR}}(m_t) - \frac{9}{2} C_{P^{1,1}_L}(m_t) - \frac{9}{4} C_{P^{1,2}_L}(m_t) + \frac{9}{4} C_{P^{1,4}_L}(m_t) \right] & \left[1 - \frac{8}{9} \left(\frac{\alpha_s(M_W)}{\alpha_s(m_t)} \right)^{\frac{2}{23}} \right] \\ \left. - \frac{1}{4} C_{P^4_L}(m_t) + \frac{9}{23} 16\pi^2 C_{W^1_L}(m_t) \left[1 - \frac{\alpha_s(m_t)}{\alpha_s(M_W)} \right] \right\} - \frac{23}{36}. \end{aligned} \tag{18}$$

Since they are expressed by coefficients of operators at $\mu = m_t$ and QCD coupling α_s, it is convenient to utilize these formula.

If the QCD corrections from m_{top} to M_W are ignored (by setting $\alpha_s(m_t) = \alpha_s(M_W)$ in eqn.(17),(18)), the above results(17)(18) would reduce to the previous results[5, 15] exactly, where the top quark and W bosons are integrated out together:

$$C_7(M_W) = -\frac{1}{2}A(x) - \frac{1}{6}\left(\frac{v_2}{v_1}\right)^2 A(y) + \xi' B(y) \quad (19)$$

$$C_8(M_W) = -\frac{1}{2}D(x) - \frac{1}{6}\left(\frac{v_2}{v_1}\right)^2 D(y) + \xi' E(y), \quad (20)$$

with A(x), B(y), D(x), E(y) defined in ref.[5].

The effects of QCD corrections to $C_7(M_W)$ and $C_8(M_W)$ can easily be seen from Fig.5 and Fig.6. Here W boson mass is taken as $M_W = 80.22$GeV, The top quark mass $m_t = 174$GeV, and the QCD scale is taken as $\Lambda^{f=5}_{QCD} = 175$ MeV[23], $M_{H^{+-}} = 300GeV$. The results of model I is displayed in Fig.5. Except for small values of v_2/v_1, $C_7(M_W)$ and $C_8(M_W)$ are both suppressed by QCD corrections from m_t to M_W. At $v_2/v_1 = 10$, $C_7(M_W)$ is suppressed 17% and $C_8(M_W)$ 12%. Fig.6 gives results calculated in model II, the differences are that $|C_7(M_W)|$ and $|C_8(M_W)|$ are both enhanced by QCD corrections for all values of v_2/v_1. At small values of v_2/v_1, $|C_7(M_W)|$ is enhanced 10%, $|C_8(M_W)|$ is enhanced 8%. Since $C_7(M_W)$ and $C_8(M_W)$ are both the input of the following QCD running from M_W to m_b, It is expected to change the final result.

The running of the coefficients of operators from $\mu = M_W$ to $\mu = m_b$ was well described in ref.[8, 10]. After this running we have the coefficients of operators at $\mu = m_b$ scale. Here $m_b = 4.9$GeV is used. Except small values of v_2/v_1, both $C_7(m_b)$ and $C_8(m_b)$ calculated in model I are suppressed in comparison to values obtained by ref.[5, 24], where the QCD running from m_t to M_W is neglected. While in model II both $|C_7(m_b)|$ and $|C_8(m_b)|$ are enhanced.

4 The $\overline{B} \to X_s\gamma$ decay rate

The leading order $b \to s\gamma$ matrix element of H_{eff} is given by the sum of operators O_5, O_6 and O_7 in our effective theory[8, 10],

$$< H_{eff} >= -2\sqrt{2}G_F V_{ts}^* V_{tb} \{C_7(\mu) + Q_d[C_5(\mu) + 3C_6(\mu)]\} < |O_7| > . \tag{21}$$

Therefore, the sought amplitude will be proportional to the squared modulus of

$$C_7^{eff}(m_b) = C_7(m_b) + Q_d \left[C_5(m_b) + 3C_6(m_b)\right] \tag{22}$$

instead of $|C_7(m_b)|^2$ itself.

Following ref.[5, 8, 10],

$$BR(\overline{B} \to X_s\gamma)/BR(\overline{B} \to X_c e\overline{\nu}) \simeq \Gamma(b \to s\gamma)/\Gamma(b \to ce\overline{\nu}). \tag{23}$$

Then applying eqs.(21),(22), one finds

$$\frac{BR(\overline{B} \to X_s\gamma)}{BR(\overline{B} \to X_c e\overline{\nu})} \simeq \frac{6\alpha_{QED}}{\pi g(m_c/m_b)} |C_7^{eff}(m_b)|^2 \left(1 - \frac{2\alpha_s(m_b)}{3\pi} f(m_c/m_b)\right)^{-1}, \tag{24}$$

where $g(m_c/m_b) \simeq 0.45$ and $f(m_c/m_b) \simeq 2.4$ corresponding to the phase space factor and the one-loop QCD correction to the semileptonic decay, respectively[25]. The electromagnetic fine structure constant evaluated at the b quark scale takes value as $\alpha_{QED}(m_b) = 1/132.7$. Afterwards one obtains the $\overline{B} \to X_s\gamma$ decay rate normalized to the quite well established semileptonic decay rate. If we take experimental result $Br(\overline{B} \to X_c e\overline{\nu}) = 10.8\%$[23], the branching ratios of $\overline{B} \to X_s\gamma$ is found.

The decay results are summarized in Fig.7 and Fig.8 as functions of v_2/v_1, with different charged Higgs mass 170GeV, 300GeV, 600GeV and 900GeV. The CLEO upper limit is also shown as a solid line.

For 2-Higgs doublet model I, the decay rates including QCD running from m_t to M_W are suppressed except small values of v_2/v_1. At $v_2/v_1 = 10$, $m_{H^{+-}} = 300GeV$, the suppression is 23%. As $v_2/v_1 \to 0$, this kind of model goes back to SM. In this small v_2/v_1 region, the QCD corrections give 7% enhancement which corresponding to SM case[21]. Therefore, the restrictions to this model parameters are less tight than previous predictions especially for large values of v_2/v_1. In Fig.7, one can see that, for lower mass of charged Higgs, small values of v_2/v_1 are still allowed. The parameter space is still open. The decay channel $t \to b\phi$ can still exist for a wide region.

The decay rates in 2-Higgs doublet model II are enhanced up to 5% more than previous calculations when charged Higgs mass is lower than 800 GeV. Although this percentage is not very large, the absolute values of the decay rates are sure higher. In Fig.8, one can easily see that, as charged Higgs mass lower than 700GeV, all values of v_2/v_1 are excluded by CLEO's $b \to s\gamma$ experiments. For larger charged Higgs mass, small value of v_2/v_1 is still allowed. It is obvious that, the top decay channel $t \to b\phi$ is already ruled out in this kind of 2-Higgs doublet model.

In the Supersymmetry model, the Higgs sector is the same as model II, but the large chargino contribution cancels much the charged Higgs contribution[26]. There is sure a suppression of decay rates from 2-Higgs doublet model II. The magnitude is more complicated, since it depends on various Supersymmetry models and chargino mass. When chargino mass is of order O(m_{top}) or higher, it should be integrated out at $\mu = m_{top}$; if it is of order O(M_W) or lower, it should be integrated out at $\mu = M_W$ scale. Further more, for a complete Supersymmetry calculation, there are also contributions from other SuSy particles which need a detailed calculation[27].

5 Conclusion

As a conclusion, we have given the full leading log QCD corrections(including QCD running from m_{top} to M_W) to $b \to s\gamma$ decay in 2-kind 2-Higgs doublet models.

The QCD running from m_t to M_W suppresses the $b \to s\gamma$ decay rate in model I, and enhances the decay rate in model II.

Although this result is not quite different from the previous calculations, our improvements lie in reducing some theoretical uncertainties. After these changes, restrictions from $b \to s\gamma$ decay to 2-Higgs doublet model parameters are less strict in model I and more tight in model II than previous predictions. It is shown that the decay $b \to s\gamma$ is by far the most restrictive process in constraining the parameters of the charged Higgs boson sector in 2-Higgs doublet model.

Note added:

After this paper was submitted for publication, the paper[28] by H. Anlauf came to our attention; the author studied the supersymmetric contributions as well as charged Higgs contributions in 2HD model II. Our results consist of 2-kinds of 2HD models; and agree with their result of model II at leading order(M_W/m_t, m_H/m_t). Further more, we also included high order contribution which can not be neglected(In ref.[28], this was picked up later after running to M_W scale to match onto results without QCD running from m_t to M_W).

Acknowledgement

The author thanks Prof. X.Y. Li, Z.M. Qiu, Z.X. Zhang, and Dr. Y.Q. Chen, Q.H. Zhang for helpful discussions.

References

[1] J.L. Hewett, SLAC preprint, SLAC-PUB-6521, 1994; and references therein.

[2] R. Ammar, et al. CLEO Collaboration, Phys. Rev. Lett. **71** (1993) 674.

[3] E. Thorndike, CLEO Collaboration, talk given at the *1993 Meeting of the American Physical Society*, Washington, D.C., April, 1993.

[4] J.L. Hewett, Phys. Rev. Lett. **70** (1993) 1045; V. Barger, M.S. Berger and R.J.N. Phillips, Phys. Rev. Lett. **70** (1993) 1368; N. Oshimo, Nucl. Phys. **B404** (1993) 20; M.A. Diaz, Phys. Lett. **B304** (1993) 278; Ali and G. Greub, preprint, DESY 93-065, ZU-TH 11/19, 1993; F.M. Borzumati, Z. Phys. **C63** (1994) 291; A.J. Buras M. Misiak, M. Münz, S. Pokorski, Nucl. Phys. **B424** (1994) 374; and references therein.

[5] B. Grinstein, R. Springer and M.B. Wise, Phys. Lett. **B202** (1988) 138; Nucl. Phys. **B339** (1990) 269.

[6] R. Grigjanis, P.J. O'Donnell, M. Sutherland, H, Navelet, Phys. Lett. **B213** (1988) 355; ibid. **B286** 413(E).

[7] G. Cella, G. Curci, G. Ricciardi, A. Vicere, Phys. Lett. **B248** (1990) 181; ibid. **B325** (1994) 227.

[8] M. Misiak, Phys. Lett. **B269** (1991) 161; Nucl. Phys. **B393** (1993) 23.

[9] K. Adel, Y.P. Yao, Mod. Phys. Lett. **A8** (1993) 1679; Phys. Rev. **D49** (1994) 4945.

[10] M. Ciuchini, E. Franco, G. Martinelli, L. Reina, L. Silvestrini, Phys. Lett. **B316** (1993) 127; M. Ciuchini, E. Franco, L. Reina, L. Silvestrini, Nucl. Phys. **B421** (1994) 41.

[11] A.J. Buras, M. Jamin, M.E. Lautenbacher and P.H. Weisz, Nucl. Phys. **B370** (1992) 69, Addendum, ibid. **B375** (1992) 501; **B400** (1993) 37 and **B400** (1993) 75.

[12] M. Ciuchini, E. Franco, G. Martinelli, L. Reina, Phys. Lett. **B301** (1993) 263; Nucl. Phys. **B415** (1994) 403.

[13] B. Grinstein, and M.B. Wise, Phys. Lett. **B201** (1988) 274.

[14] W.S Hou and R.S. Willey, Phys. Lett. **B202** (1988)591.

[15] S. Bertolini, F. Borzumati, A. Masiero and G. Ridolfi, Nucl. Phys. **B353** (1991) 591.

[16] F. Abe, et al. CDF Collaboration, Phys. Rev. Lett. **73** (1994) 225.

[17] H.E. Haber, G.L. Kane and T. Sterling, Nucl. Phys. **B161** (1979) 493.

[18] S.L. Glashow and S. Weinberg, Phys. Rev. **D15** (1977) 1958.

[19] L. Abbott, Nucl. Phys. **B185** (1981) 189.

[20] P. Cho, B. Grinstein, Nucl. Phys. **B365** (1991) 279.

[21] C.S. Gao, J.L. Hu, C.D. Lü, Z.M. Qiu, preprint CCAST 93-28, hep-ph/9408351.

[22] H.D. Politzer, Nucl. Phys. **B172** (1980) 349; H. Simma, preprint, DESY 93-083.

[23] Particle Data Group, Phys. Rev. **D45** (1992) No.11.

[24] M. Ciuchini, E. Franco, G. Martinelli, L. Reina, L. Silvestrini, preprint, CERN-TH-7283/94, ROME prep. 94/1020, ULB-TH 09/94.

[25] N. Cabibbo and L. Maiani, Phys. Lett. **B79** (1978) 109.

[26] R. Barbieri and G.F. Giudice, Phys. Lett. **B309** (1993) 86.

[27] Cai-dian Lü, in preparation.

[28] H. Anlauf, Nucl. Phys. **B430** (1994) 245.

Figure Captions

Fig.1 Leading order matching conditions at the top quark scale for the 1PI Green functions in the full theory and in the intermediate effective field theory.

Fig.2 One loop matching conditions at the top quark scale for the 1PI Green functions in the full theory and in the intermediate effective field theory.

Fig.3 One of the Feynman diagram in calculating anomalous dimensions, with the heavy dot denoting high dimension operator.

Fig.4 Matching conditions at $\mu = M_W$ for four quarks and two quarks 1PI Green functions in the intermediate effective field theory and effective field theory below W scale.

Fig.5 The photon and gluon magnetic moment operator's coefficients $C_7(M_W)$ and $C_8(M_W)$ in model I. The solid lines are our QCD corrected results, the other two are uncorrected ones.

Fig.6 The photon and gluon magnetic moment operator's coefficients $C_7(M_W)$ and $C_8(M_W)$ in model II. The solid lines are our QCD corrected results, the other two are uncorrected ones.

Fig.7 BR($\overline{B} \to X_s\gamma$) of model I as function of v_2/v_1 for different charged Higgs masses. The solid line is the upper limit of CLEO. This line upper is the excluded region.

Fig.8 BR($\overline{B} \to X_s\gamma$) in model II as function of v_2/v_1 for different charged Higgs masses. The solid line is the upper limit of CLEO.

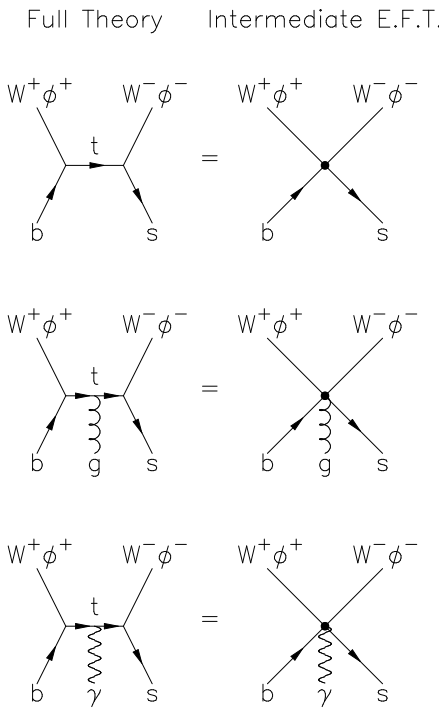

Fig. 1

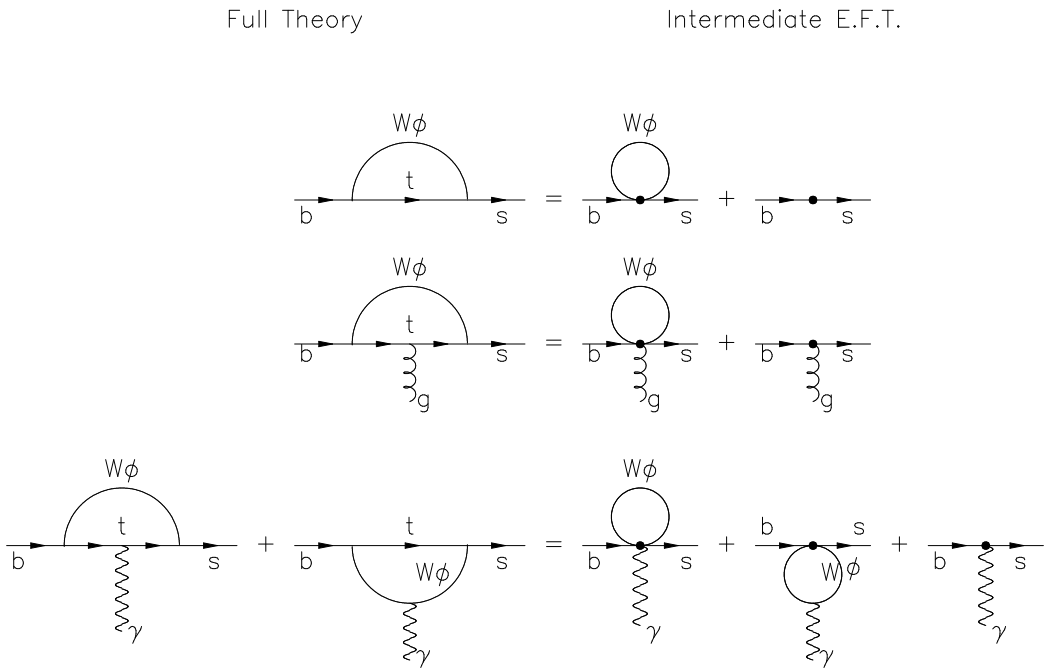

Fig. 2

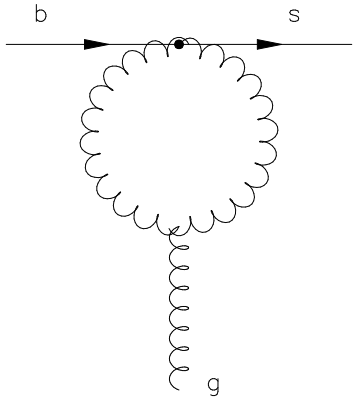

Fig. 3

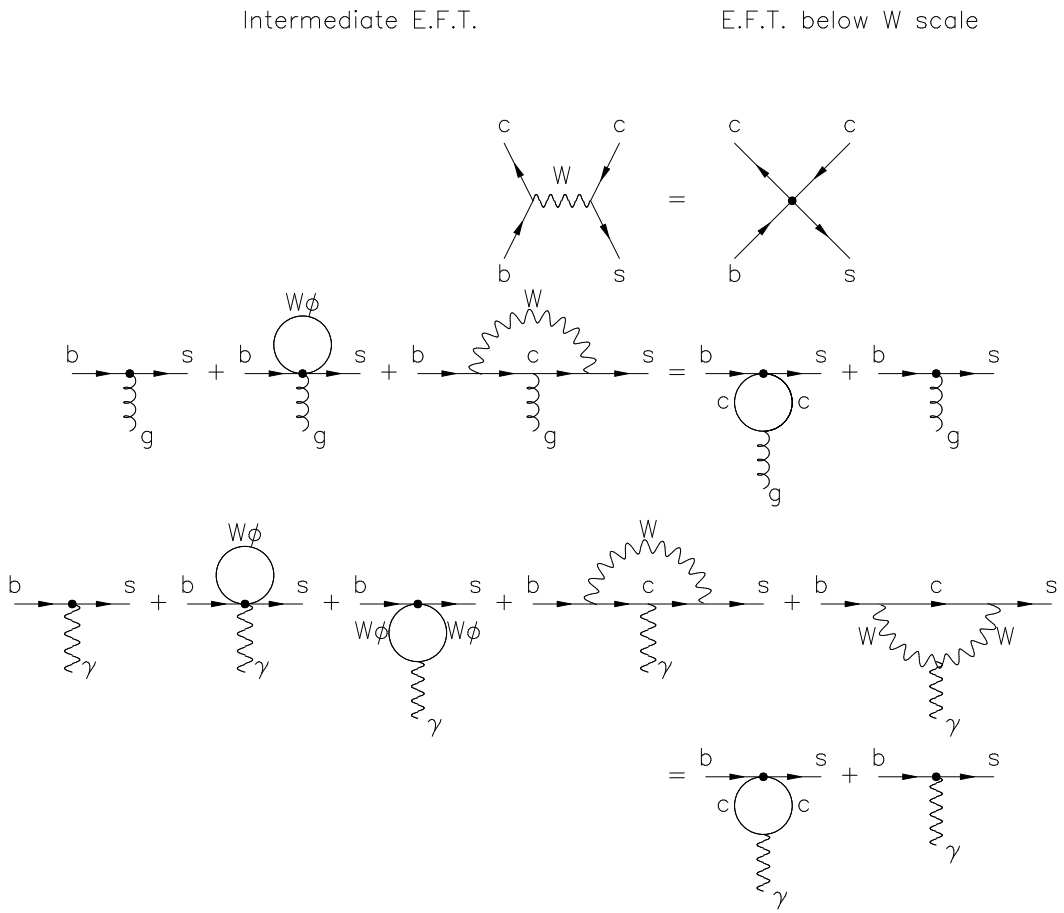

Fig. 4

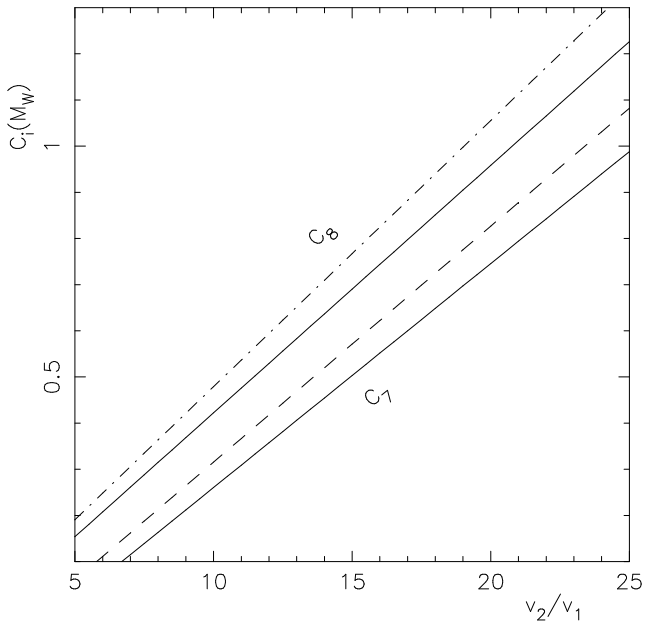
$C_i(M_W)$
1
0.5
C_8
C_7
5
10
15
20
25
v_2/v_1

Fig. 5

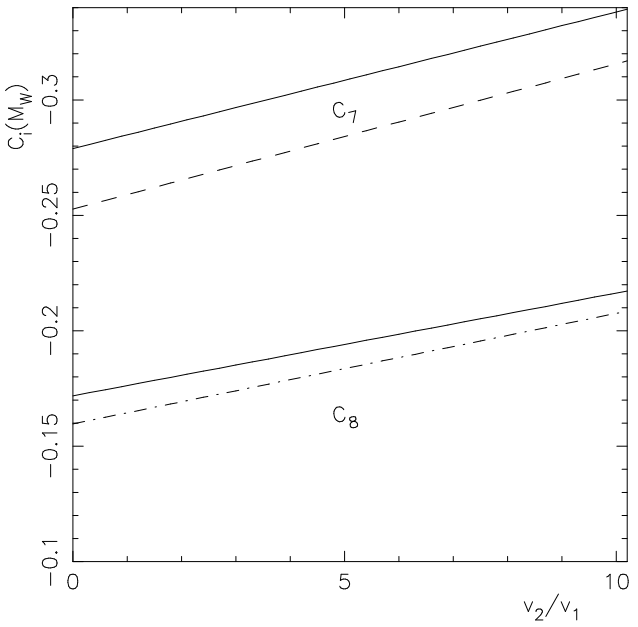
$C_i(M_W)$
−0.3
−0.25
−0.2
−0.15
−0.1
C_7
C_8
0
5
10
v_2/v_1

Fig. 6

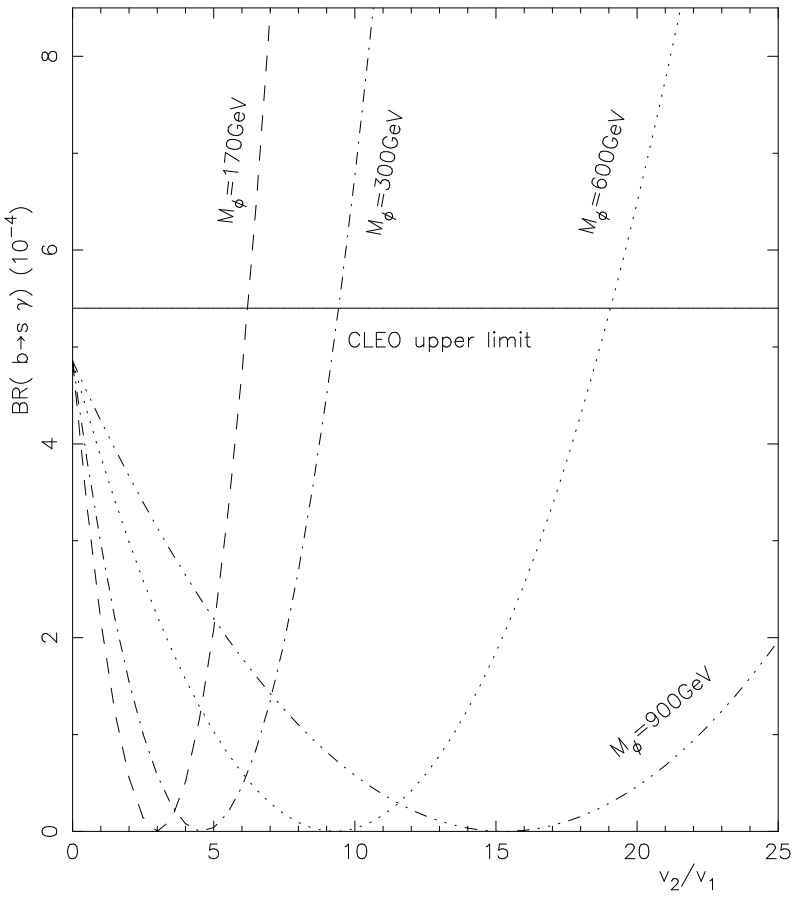
BR(b→s γ) (10^{-4})
v_2/v_1
M_ϕ=170GeV
M_ϕ=300GeV
M_ϕ=600GeV
M_ϕ=900GeV
CLEO upper limit
0
2
4
6
8
0
5
10
15
20
25

Fig. 7

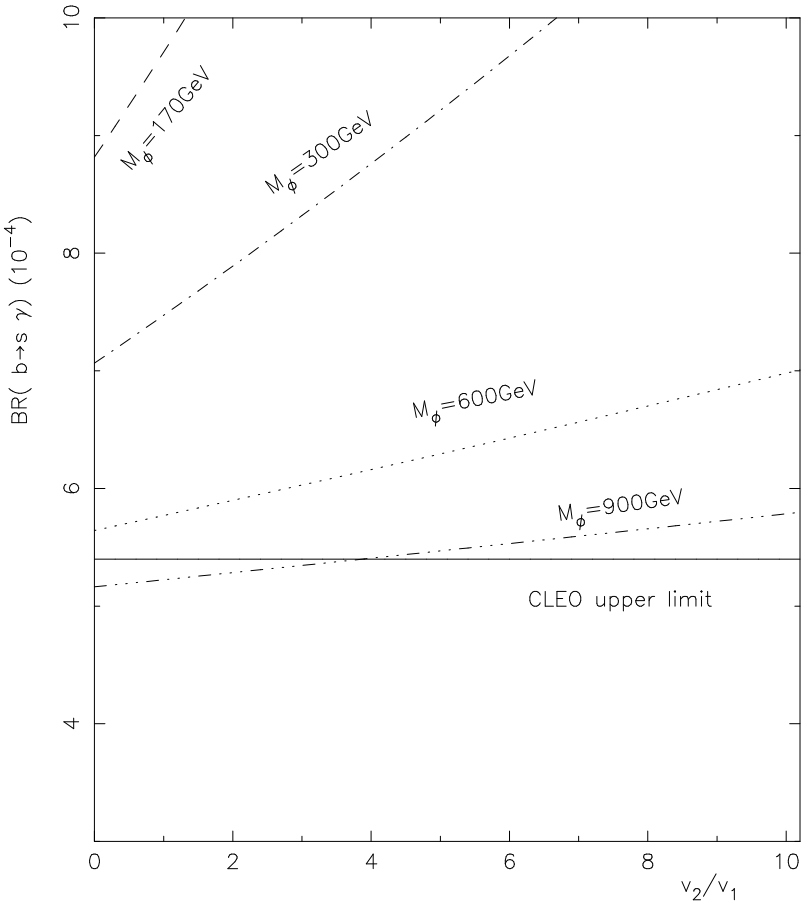
BR(b→s γ) (10^{-4})
v_2/v_1
M_ϕ=170GeV
M_ϕ=300GeV
M_ϕ=600GeV
M_ϕ=900GeV
CLEO upper limit
4
6
8
10
0
2
4
6
8
10

Fig. 8